

Weyl semimetal on the pyrochlore lattice

C. Berke, C. Timm



TECHNISCHE
UNIVERSITÄT
DRESDEN

May 19, 2017

Weyl semimetals

- Hermann Weyl (1929): simplified version of Dirac equation:

$$i(\partial_0 - \boldsymbol{\sigma} \cdot \boldsymbol{\nabla})\psi_L = 0$$

- TWS provide the first ever realization of Weyl fermions
- 3D gapless system with topological properties
- point touchings of nondegenerate conduction and valence bands

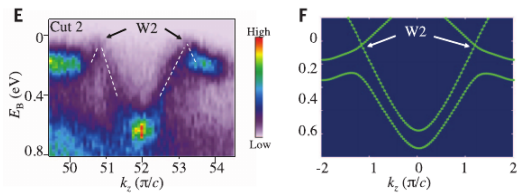


Figure: Weyl cones in TaAs (Xu *et al.*, Science 349 (6248), 613-617)

- band structure near Weyl points (WP): $H_{\text{Weyl}} = v_{ij} k_i \sigma_j$

Weyl semimetals

- Weyl points are stable objects (all σ_i appear in H_{Weyl})
- topological invariant for WP: chirality $\chi = 1/2\pi \int_S d\mathbf{S} \cdot \mathbf{B}(\mathbf{k})$

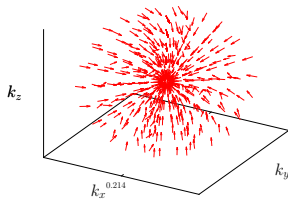
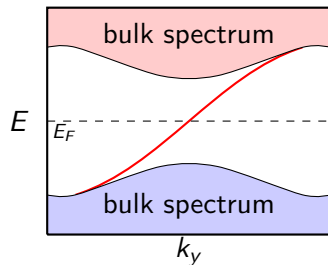
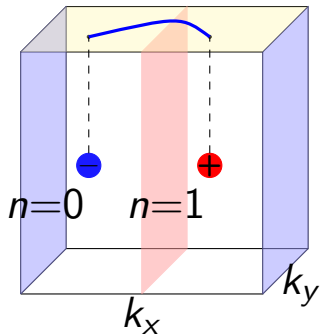


Figure: hedgehog in momentum space / magnetic monopole

- WPs always appear in pairs of opposite chirality
- chiral anomaly, negative magnetoresistance, ...
- first observation of Weyl fermions in TaAs (*Lu et al. Science 349, 622-624, 2015*)

Surface states & Fermi arcs

- TWS inherits the topology of an insulator of a lower dimension
- TWS has protected surface states
- surface states form arc at the Fermi energy



Motivation & Overview

- Why pyrochlore iridates ?

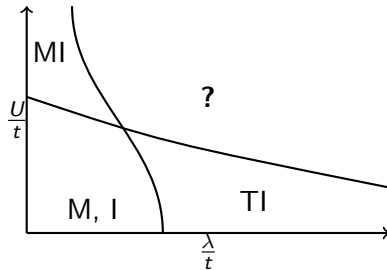
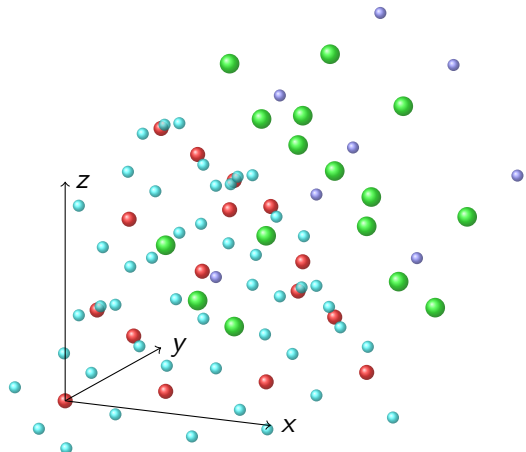


Figure: Annu. Rev. Condens. Matter Phys. 2014, 5:57-82

- SOC and U have same order of magnitude ($5d$ electrons)
- Iridium-containing perovskites, osmium oxides, **pyrochlore iridates**
- General formula: $R_2\text{Ir}_2\text{O}_7$, R - rare earth element
- Aim: Motivate model with one Kramers doublet at each Ir site

Lattice structure

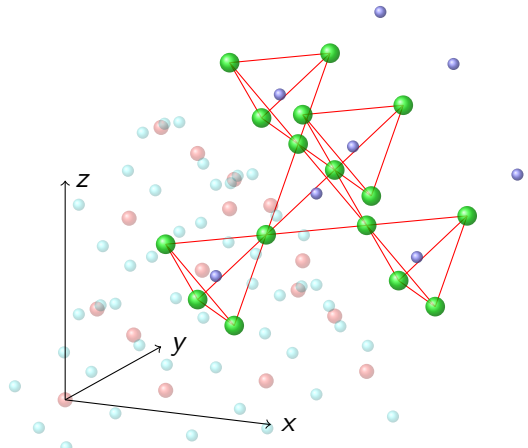
- 4 nonequivalent atomic positions: $R_2\text{Ir}_2\text{O}_6\text{O}'$
- R_4 and Ir_4 tetrahedra + oxygen environment
- one structural parameter: oxygen x-parameter



- Ir atoms:
pyrochlore lattice
- 6 NN + 12 NNN

Lattice structure

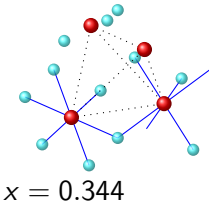
- 4 nonequivalent atomic positions: $R_2\text{Ir}_2\text{O}_6\text{O}'$
- R_4 and Ir_4 tetrahedra + oxygen environment
- one structural parameter: oxygen x-parameter



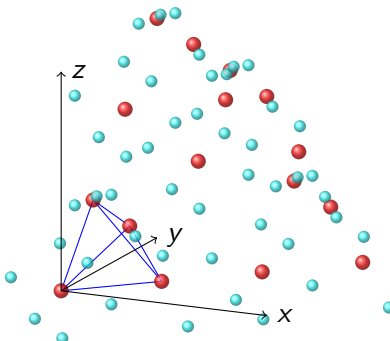
- Ir atoms:
pyrochlore lattice
- 6 NN + 12 NNN

Lattice structure

- 4 nonequivalent atomic positions: $R_2\text{Ir}_2\text{O}_6\text{O}'$
- R_4 and Ir_4 tetrahedra + oxygen environment
- one structural parameter: oxygen x-parameter

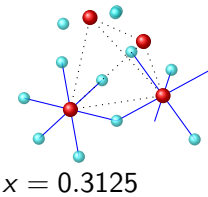


- Ir atoms:
pyrochlore lattice
- 6 NN + 12 NNN

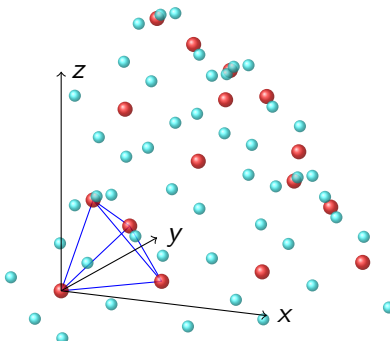


Lattice structure

- 4 nonequivalent atomic positions: $R_2\text{Ir}_2\text{O}_6\text{O}'$
- R_4 and Ir_4 tetrahedra + oxygen environment
- one structural parameter: oxygen x-parameter

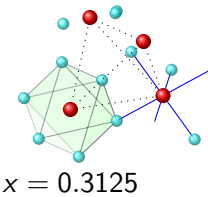


- Ir atoms:
pyrochlore lattice
- 6 NN + 12 NNN

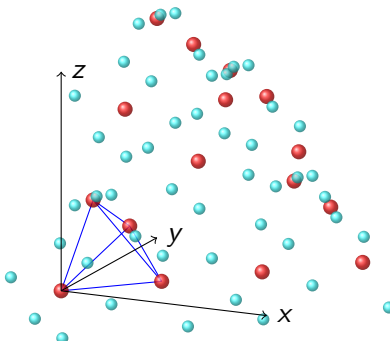


Lattice structure

- 4 nonequivalent atomic positions: $R_2\text{Ir}_2\text{O}_6\text{O}'$
- R_4 and Ir_4 tetrahedra + oxygen environment
- one structural parameter: oxygen x-parameter

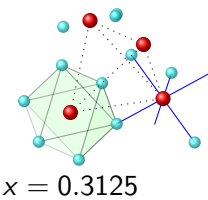


- Ir atoms:
pyrochlore lattice
- 6 NN + 12 NNN

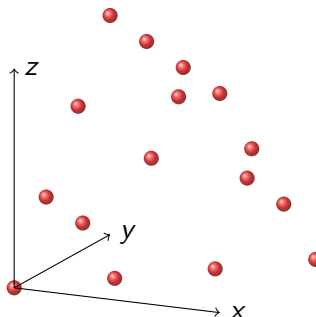


Lattice structure

- 4 nonequivalent atomic positions: $R_2\text{Ir}_2\text{O}_6\text{O}'$
- R_4 and Ir_4 tetrahedra + oxygen environment
- one structural parameter:
oxygen x-parameter

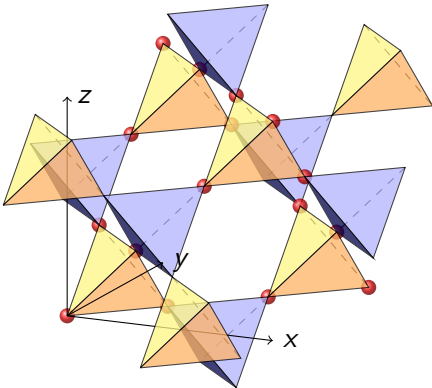
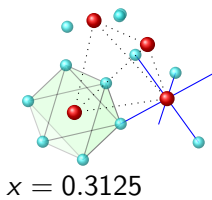


- Ir atoms:
pyrochlore lattice
- 6 NN + 12 NNN



Lattice structure

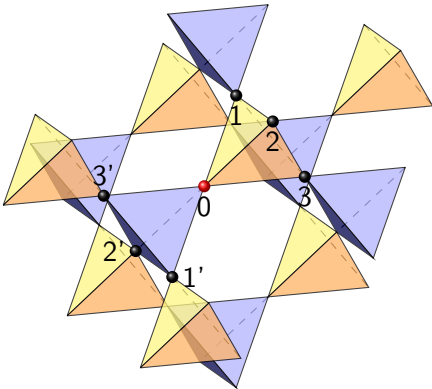
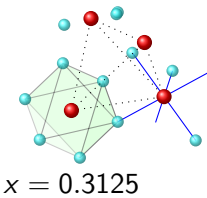
- 4 nonequivalent atomic positions: $R_2\text{Ir}_2\text{O}_6\text{O}'$
- R_4 and Ir_4 tetrahedra + oxygen environment
- one structural parameter: oxygen x-parameter



- Ir atoms:
pyrochlore lattice
- 6 NN + 12 NNN

Lattice structure

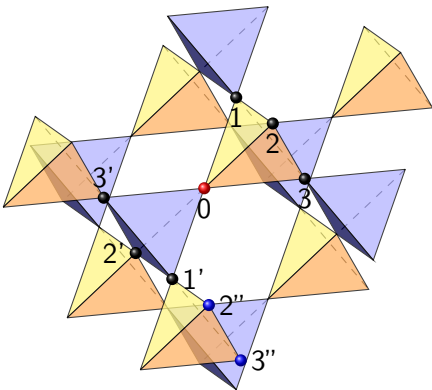
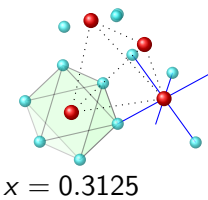
- 4 nonequivalent atomic positions: $R_2\text{Ir}_2\text{O}_6\text{O}'$
- R_4 and Ir_4 tetrahedra + oxygen environment
- one structural parameter: oxygen x-parameter



- Ir atoms:
pyrochlore lattice
- 6 NN + 12 NNN

Lattice structure

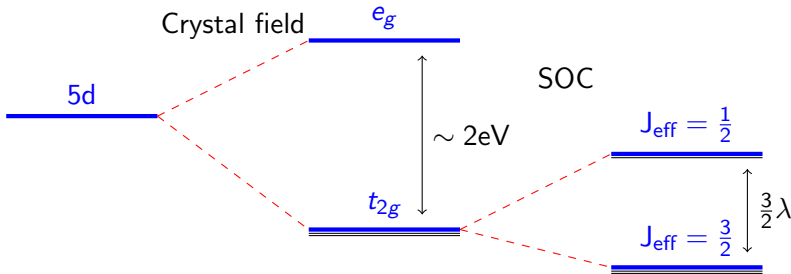
- 4 nonequivalent atomic positions: $R_2\text{Ir}_2\text{O}_6\text{O}'$
- R_4 and Ir_4 tetrahedra + oxygen environment
- one structural parameter: oxygen x-parameter



- Ir atoms:
pyrochlore lattice
- 6 NN + 12 NNN

Effective $J = 1/2$ picture

- el. configuration: $[\text{Xe}] 4f^{14} 5d^7 6s^2$, here: $\text{Ir}^{4+} \Rightarrow 5 d\text{-electrons}$



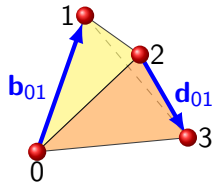
- crystal field splits the d-levels in e_g doublet and t_{2g} triplet
- $\mathcal{P}_{t_{2g}} \mathbf{L} \mathcal{P}_{t_{2g}} = -\mathbf{L}_{\text{eff}} \Rightarrow t_{2g}$ electrons are “pseudo” p electrons
- SOC: high-energy doublet and lower quadruplet
- local pseudo-spin state: $|J_{\text{eff}}^z = \frac{1}{2}\rangle = \frac{1}{\sqrt{3}}(|xy, \uparrow\rangle + |yz, \downarrow\rangle + i|zx, \downarrow\rangle)$

The Hamiltonian & space group symmetries

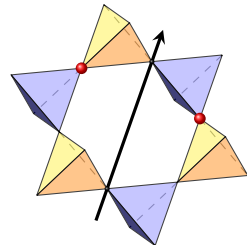
most general TRI Hamiltonian with NN & NNN hopping

$$H = \sum_{\langle i,j \rangle} c_i^\dagger (t_1 \mathbb{1} + it_2 \mathbf{d}_{ij} \cdot \boldsymbol{\sigma}) c_j + \sum_{\langle\langle i,j \rangle\rangle} c_i^\dagger [t'_1 \mathbb{1} + i(t'_2 \mathcal{R}_{ij} + t'_3 \mathcal{D}_{ij}) \cdot \boldsymbol{\sigma}] c_j$$

- *global* pseudospin basis, $c_i = (c_{i\uparrow}, c_{i\downarrow})$
- t_i , t'_i are real hopping parameters



- \mathbf{d}_{ij} aligned along the opposite bond of the tetrahedron containing i,j



- $\mathcal{R}_{ij} = \mathbf{b}_{ik} \times \mathbf{b}_{kj}$ and $\mathcal{D}_{ij} = \mathbf{d}_{ik} \times \mathbf{d}_{kj}$

H_{sym} vs. H_{micro}

microscopic model

$$H = \sum_{i,j,\sigma\sigma'} d_{i,\sigma}^\dagger \left(T_{O,\sigma\sigma'}^{ij} + T_{d,\sigma\sigma'}^{ij} \right) d_{j,\sigma'}$$

- direct hopping between local t_{2g} orbitals: π, σ, δ overlaps
- oxygen mediated hopping
- same Hamiltonian?

H_{sym} vs. H_{micro}

microscopic model

$$H = \sum_{i,j,\sigma\sigma'} d_{i,\sigma}^\dagger \left(T_{O,\sigma\sigma'}^{ij} + T_{d,\sigma\sigma'}^{ij} \right) d_{j,\sigma'}$$

- direct hopping between local t_{2g} orbitals: π, σ, δ overlaps
- oxygen mediated hopping
- same Hamiltonian? Yes!

Result (for NN-hopping)

$$t_1 = \frac{130}{243} t_{\text{oxy}} + \frac{17}{324} t_\sigma - \frac{79}{243} t_\pi - \frac{43}{972} t_\delta \quad (1)$$

$$t_2 = \frac{28}{243} t_{\text{oxy}} + \frac{15}{243} t_\sigma - \frac{40}{243} t_\pi - \frac{55}{243} t_\delta \quad (2)$$

- choose the following parameter subset (PRB 86, 155101(2013)):

- $t_{\text{oxy}} = 1, t_\pi = -\frac{2}{3} t_\sigma, \frac{t'_\sigma}{t_\sigma} = \frac{t'_\pi}{t_\pi} = 0.08, t_\delta = t'_\delta = 0$

Interacting Electrons

Add onsite Hubbard repulsion

$$H = H_{NN} + H_{NNN} + H_U, \quad \text{with } H_U = U \sum_i n_{i\uparrow} n_{i\downarrow}$$

- perform mean-field decoupling (Hartree-Fock)

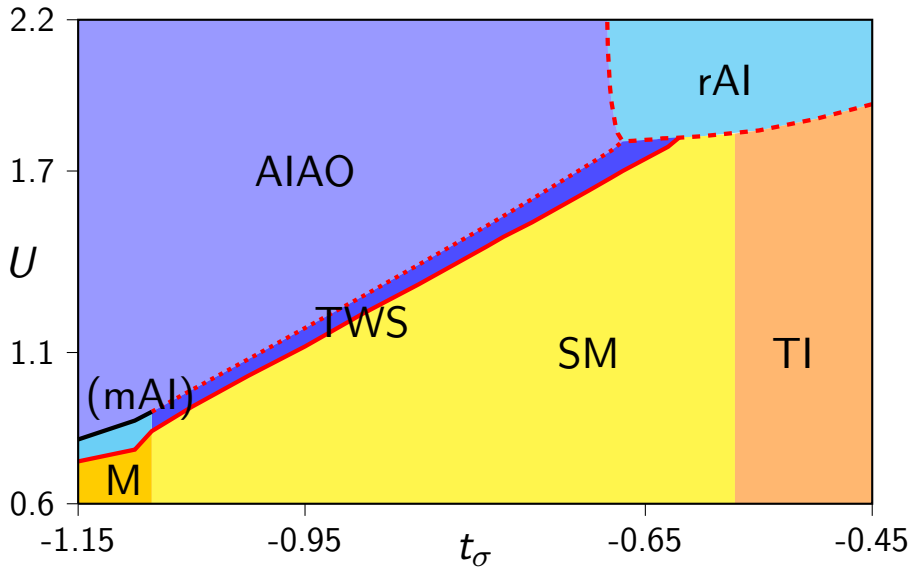
$$\begin{aligned} n_{i\uparrow} n_{i\downarrow} &\approx n_{i\uparrow} \langle n_{i\downarrow} \rangle + \langle n_{i\uparrow} \rangle n_{i\downarrow} - \langle n_{i\uparrow} \rangle \langle n_{i\downarrow} \rangle \\ &\quad - c_{i\uparrow}^\dagger c_{i\downarrow} \langle c_{i\downarrow}^\dagger c_{i\uparrow} \rangle - \langle c_{i\uparrow}^\dagger c_{i\downarrow} \rangle c_{i\downarrow}^\dagger c_{i\uparrow} + \langle c_{i\uparrow}^\dagger c_{i\downarrow} \rangle \langle c_{i\downarrow}^\dagger c_{i\uparrow} \rangle \end{aligned}$$

- mean-field parameters determine occupation numbers and $\langle \mathbf{J}_i^{\text{eff}} \rangle$:

$$\mathbf{J}_i^k = \frac{1}{2} \sum_{\alpha\beta} c_{i\alpha}^\dagger \sigma_{\alpha\beta}^k c_{i\beta}.$$

- $\langle \mathbf{J}_i^{\text{eff}} \rangle$ = local magnetic moments of the electrons
- $\langle \mathbf{J}_i^{\text{eff}} \rangle$ and $\langle n_i \rangle$ are determined self-consistently

Phase diagram



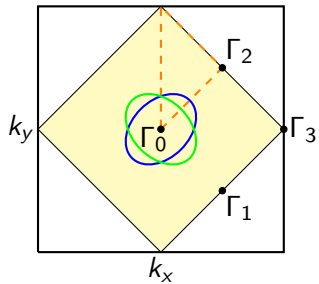
The topological insulator

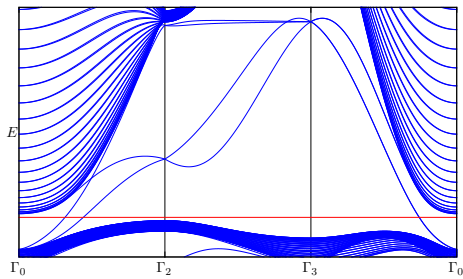
Reminder: \mathbb{Z}_2 invariants for TRI bandstructures

- characterized by four \mathbb{Z}_2 invariants (Fu, Kane, Mele PRL **98**, 106803 (2007))
- for insulators with \mathcal{I} symmetry (Fu, Kane PRB **76**, 045302 (2007)):

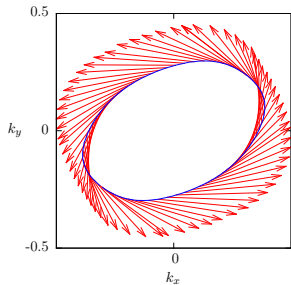
$$(-1)^\nu = \prod_{i=1}^8 \delta_i \quad \text{and} \quad \delta_i = \prod_{m=1}^2 \xi_{2m}(\Gamma_i)$$

- strong topological insulator with indices (1; 000)
- key properties:
 - surface states
 - surface is a topological metal
- here: surface in (001) direction





(a) energy spectrum for finite geometry (30 layers in (100) direction)

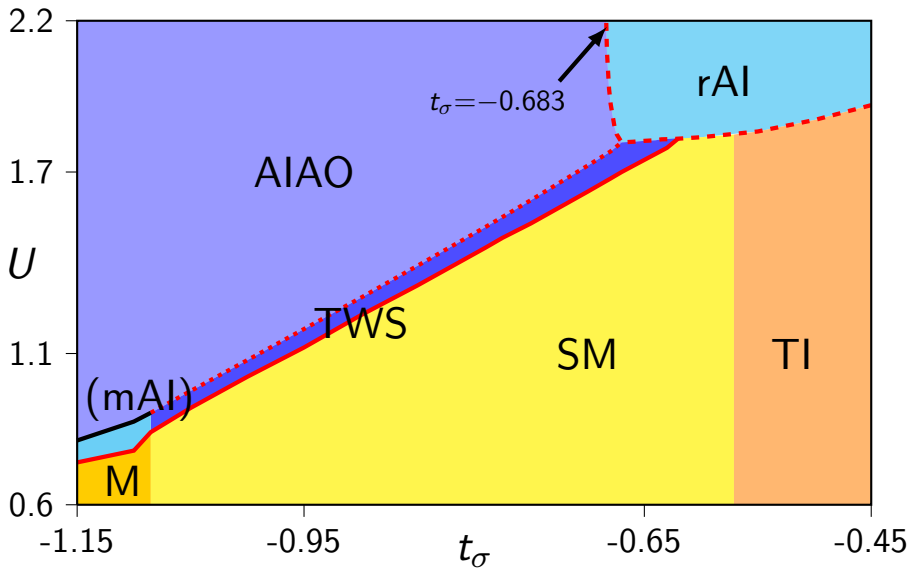


(b) $\langle \mathbf{S} \rangle$ along Fermi line

Figure: surface properties of the TI

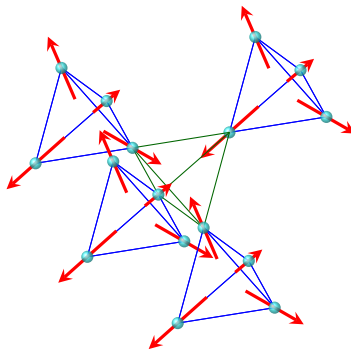
- protected surface states between Γ_0 and the other TRIM
- spin rotates with \mathbf{k} around the Fermi circle

Magnetic order



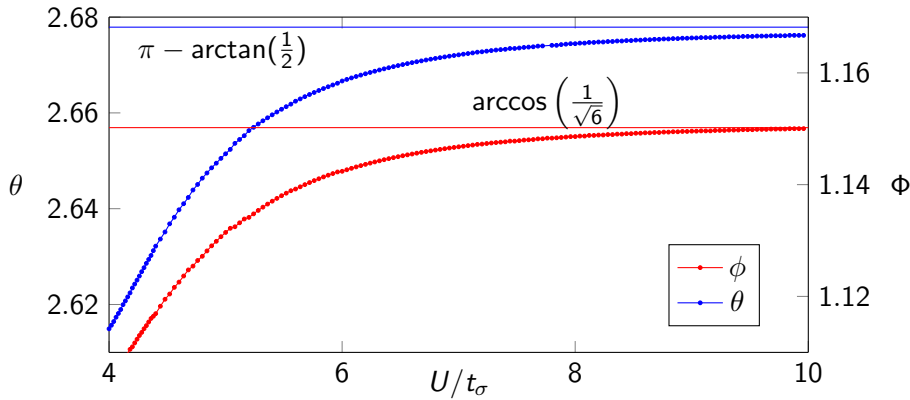
The AIAO ordering

- antiferromagnetic ordering for $U > U_c$
- mAI, AIAO, TWS: *All-in-all-out-ordering*
- breaks \mathcal{T} symmetry, but \mathcal{I} is conserved
- same order was obtained using LDA+U, DMFT, CDMFT, ...



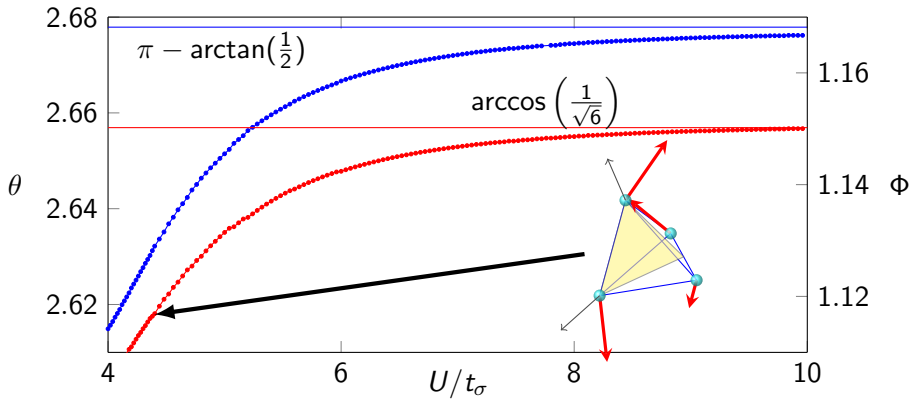
The rAI ordering

- first-order quantum phase transition
- pairwise rotation of magnetic moments



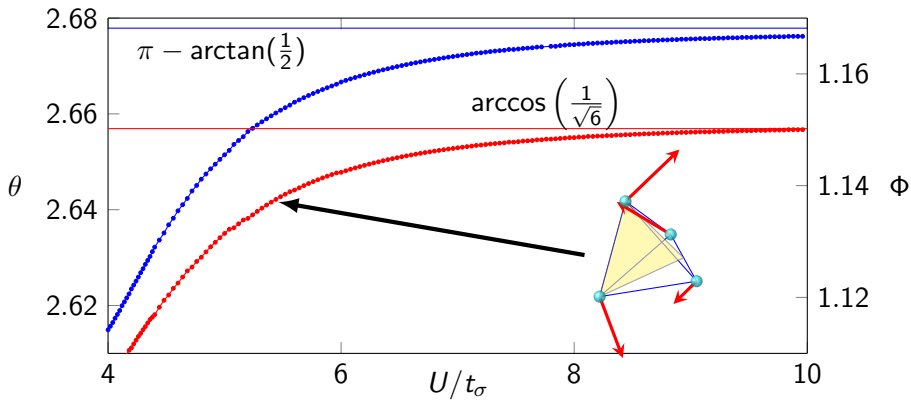
The rAI ordering

- first-order quantum phase transition
- pairwise rotation of magnetic moments



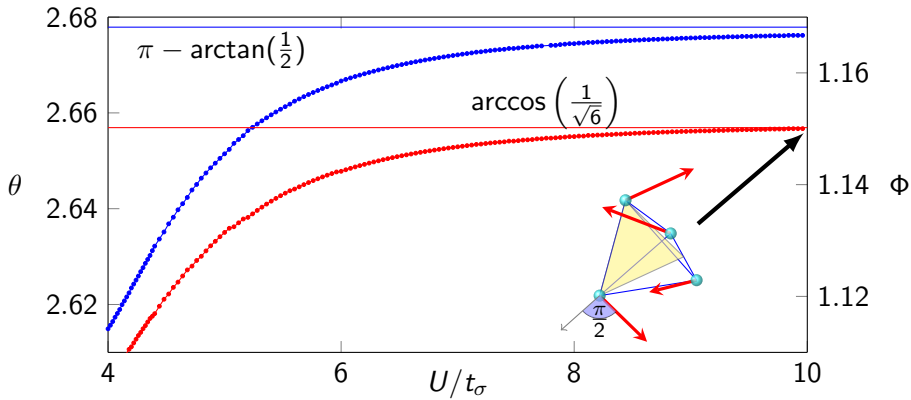
The rAI ordering

- first-order quantum phase transition
- pairwise rotation of magnetic moments



The rAI ordering

- first-order quantum phase transition
- pairwise rotation of magnetic moments

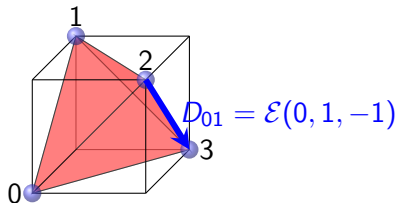


The rAI ordering

- Explanation for phase transition and new order:

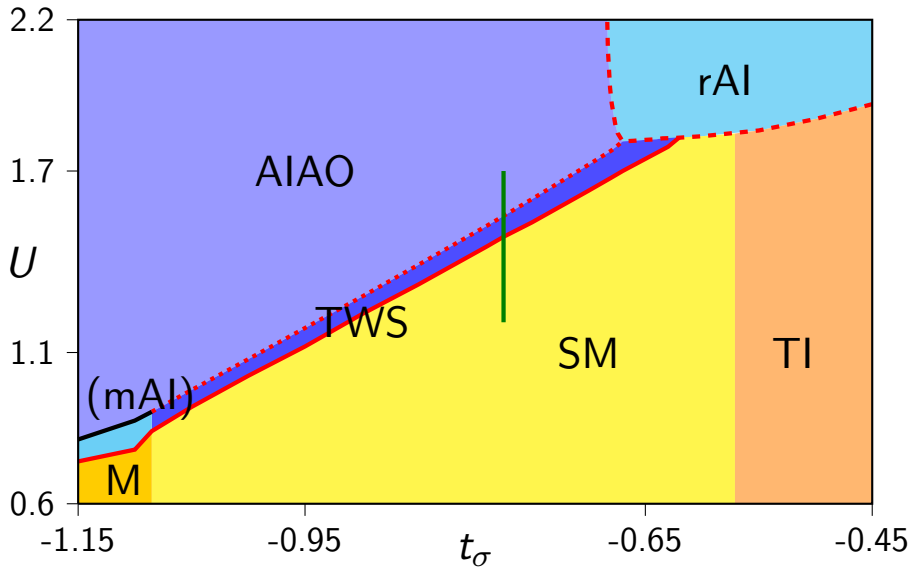
$$H = \sum_{\langle ij \rangle} \left[JS_i S_j + D_{ij}(S_i \times S_j) + S_i^a \Gamma_{ij}^{ab} S_j^b + \dots \right]$$

(Elhajal et. al PRB 71, 094420 (2010))

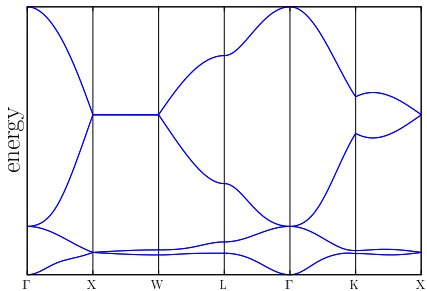


- D_{ij} (anti)parallel to opposite bond \rightarrow (in)direct DM interaction
- $E(t_\sigma)$ changes sign for $t_\sigma = -0.67$, here: $t_\sigma \approx -0.683$
- direct DMI: AIAO, indirect DMI: continuous manifold
- here: limit $t_\sigma/U \rightarrow 0$: groundstate belongs to this manifold

Evolution of the magnetization



Evolution of the magnetization



(a) semimetal

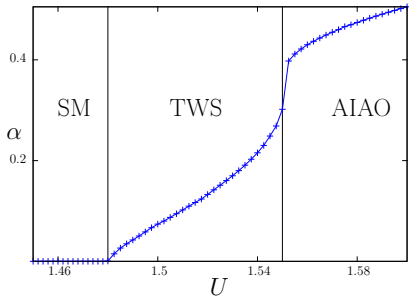
(b) evolution of α ($t_\sigma = -0.775$)

Figure: $U=0$, $t_\sigma = -0.775$

- magnetization α : $\mathbf{S}_i = \alpha/2 (\cos \varphi_i \sin \vartheta_i, \sin \varphi_i \sin \vartheta_i, \cos \vartheta_i)$
- continuous transition from SM to TWS
- magnetization "jumps" from TWS to AIAO for $-0.78 < t_\sigma < -0.68$

Evolution of the magnetization

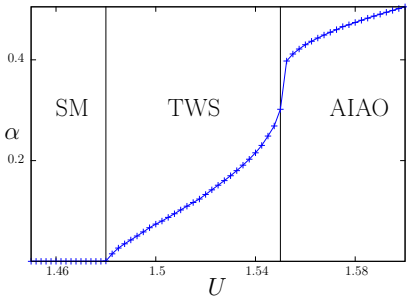
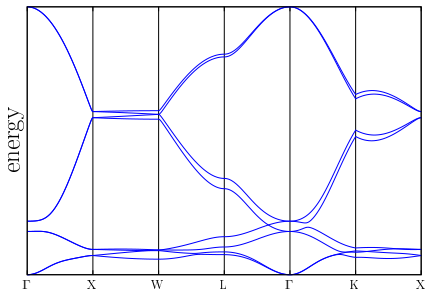
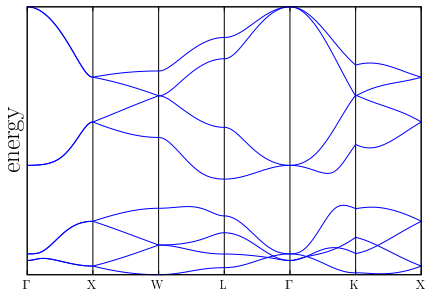


Figure: $U=1.54$, $t_\sigma = -0.775$

- magnetization α : $\mathbf{S}_i = \alpha/2 (\cos \varphi_i \sin \vartheta_i, \sin \varphi_i \sin \vartheta_i, \cos \vartheta_i)$
- continuous transition from SM to TWS
- magnetization "jumps" from TWS to AIAO for $-0.78 < t_\sigma < -0.68$

Evolution of the magnetization



(a) AIAO

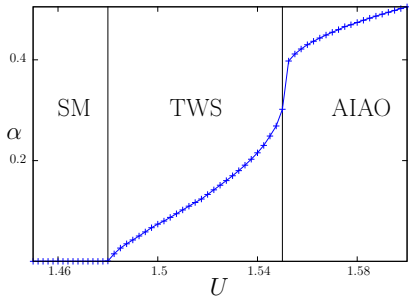
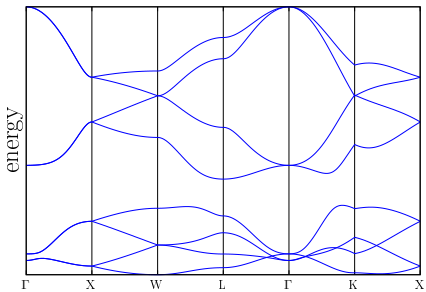
(b) evolution of α ($t_\sigma = -0.775$)

Figure: $U=1.7$, $t_\sigma = -0.775$

- magnetization α : $\mathbf{S}_i = \alpha/2 (\cos \varphi_i \sin \vartheta_i, \sin \varphi_i \sin \vartheta_i, \cos \vartheta_i)$
- continuous transition from SM to TWS
- magnetization "jumps" from TWS to AIAO for $-0.78 < t_\sigma < -0.68$

Evolution of the magnetization



(a) AIAO

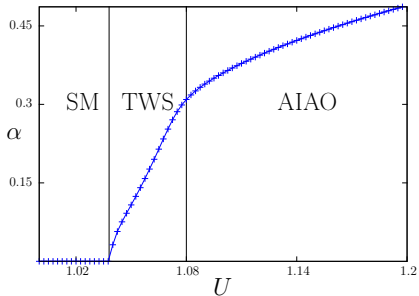
(b) evolution of α ($t_\sigma = -0.775$)

Figure: $U=1.7$, $t_\sigma = -0.775$

- magnetization α : $\mathbf{S}_i = \alpha/2 (\cos \varphi_i \sin \vartheta_i, \sin \varphi_i \sin \vartheta_i, \cos \vartheta_i)$
- continuous transition from SM to TWS
- magnetization "jumps" from TWS to AIAO for $-0.78 < t_\sigma < -0.68$

Annihilation of the Weyl points

- WP move from Γ to L
- annihilation with WP with opposite chirality

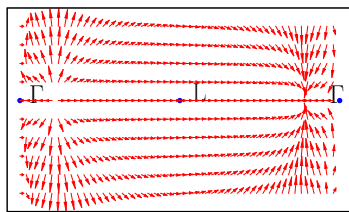
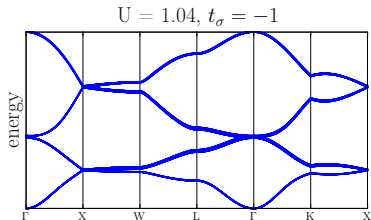
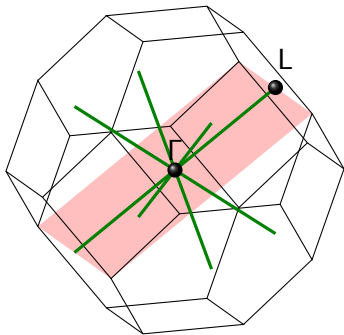
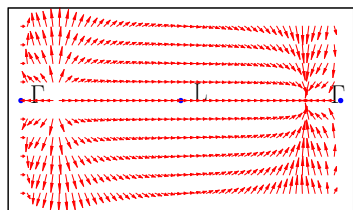
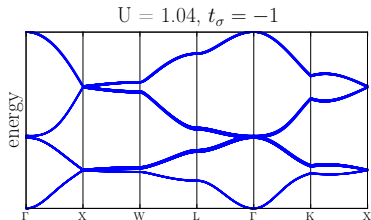
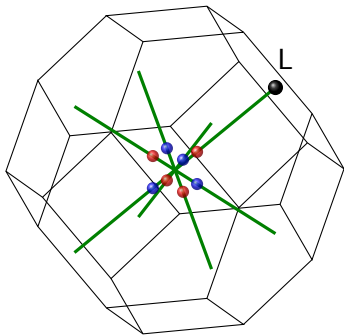


Figure: berry flux

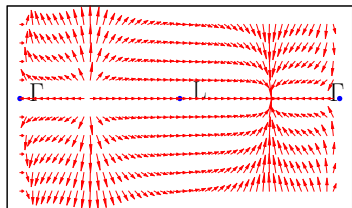
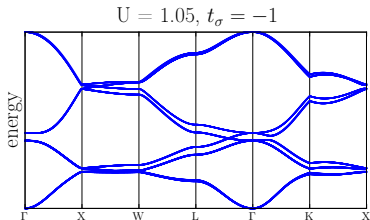
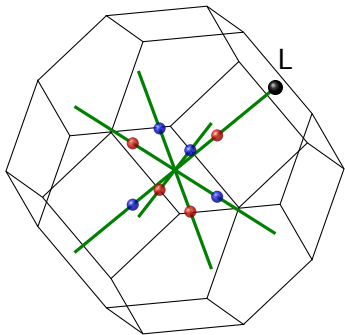
Annihilation of the Weyl points

- WP move from Γ to L
- annihilation with WP with opposite chirality



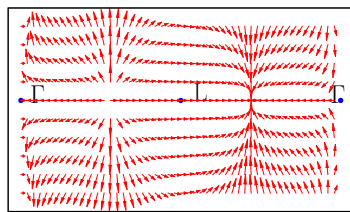
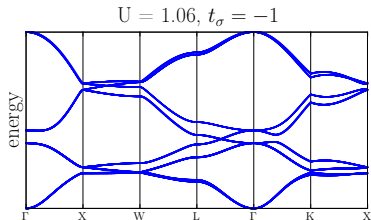
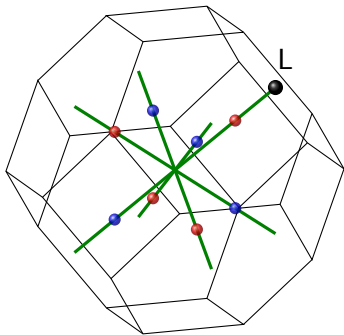
Annihilation of the Weyl points

- WP move from Γ to L
- annihilation with WP with opposite chirality



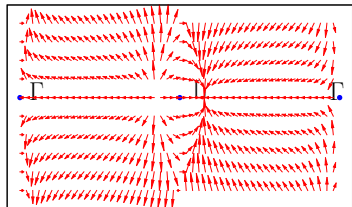
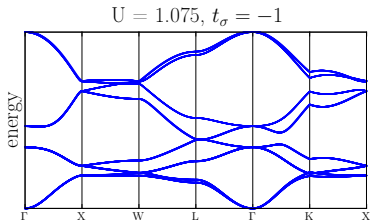
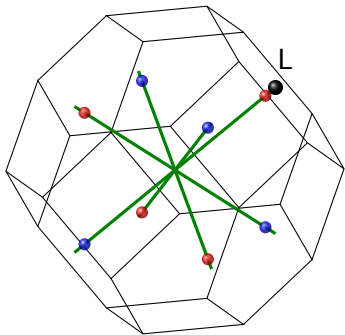
Annihilation of the Weyl points

- WP move from Γ to L
- annihilation with WP with opposite chirality



Annihilation of the Weyl points

- WP move from Γ to L
- annihilation with WP with opposite chirality



Annihilation of the Weyl points

- WP move from Γ to L
- annihilation with WP with opposite chirality

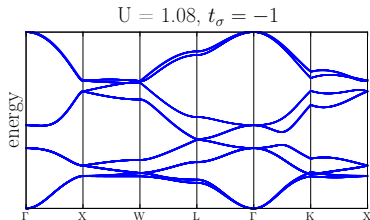
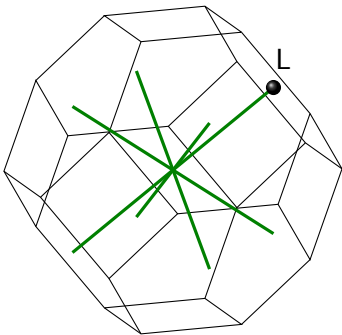


Figure: band structure

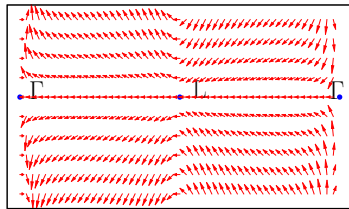
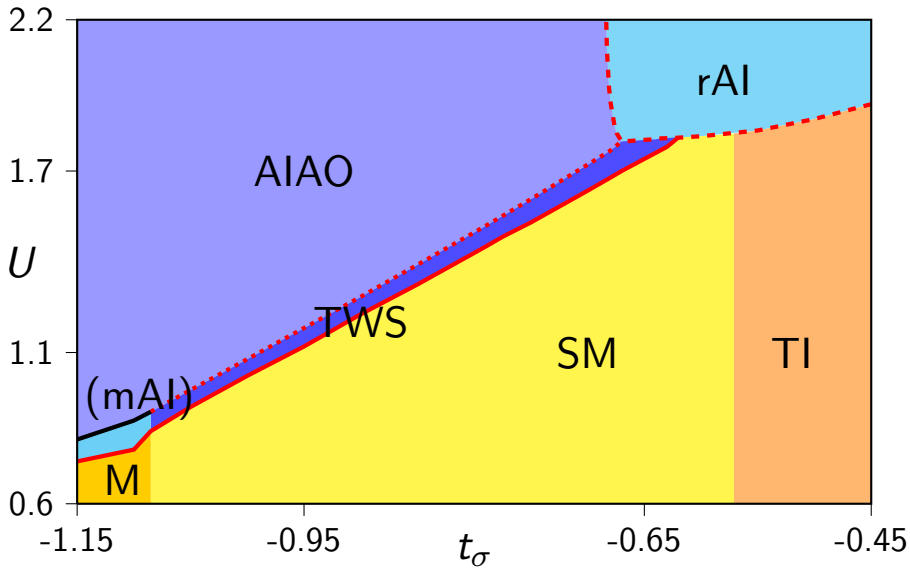


Figure: berry flux

The mAl phase



mAl or type II Weyl semimetal?

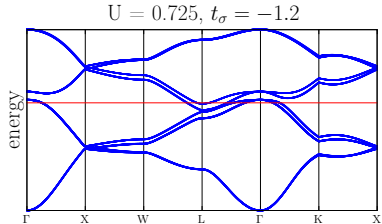
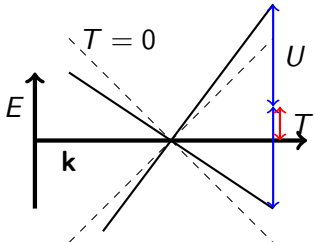


Figure: band structure for mAl phase



type II WSM (Soluyanov et al., Nature 527, 2015)

- $H(\mathbf{k}) = \sum_{\substack{i=x,y,z \\ j=0,x,y,z}} k_i v_{ij} \sigma_j$
- $\epsilon_{\pm} = \underbrace{T(\mathbf{k})}_{\text{tilts the Weyl cone}} \pm U(\mathbf{k}).$
- $T(\mathbf{k}) > U(\mathbf{k})$ for some \mathbf{k} : type II Weyl semimetal

- $T > U$ in (111)-direction
- WP touching point of electron- and holelike Fermi surfaces
- WP not at Fermi energy

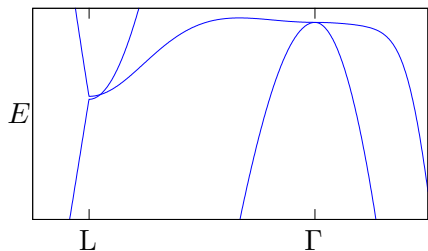
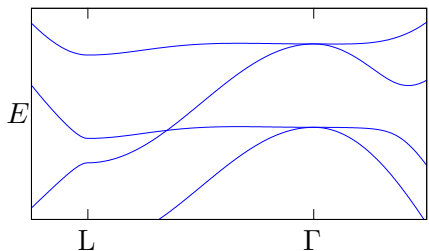
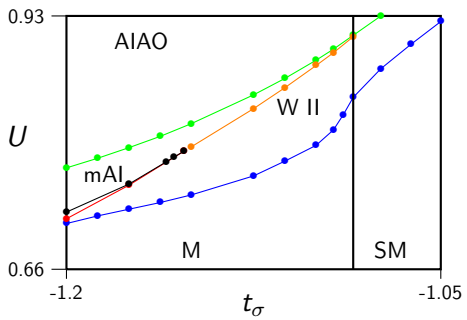


Figure: $t_\sigma = -1.1$

- additional gap closing at L
- type 2 TWS with 16 WP
- annihilation between L and Γ



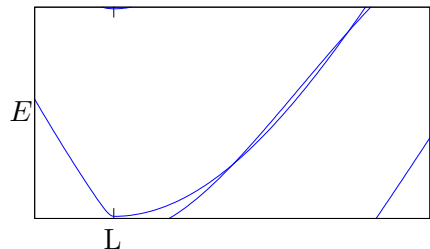
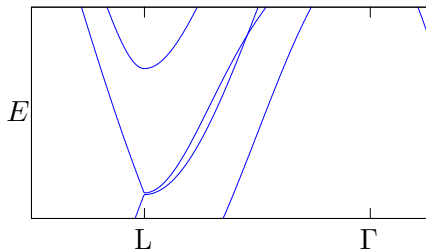
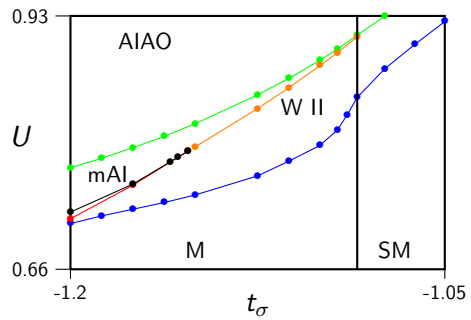


Figure: $t_\sigma = -1.2$

- additional gap closing at L
- type 2 TWS with 16 WP
- annihilation between L and Γ

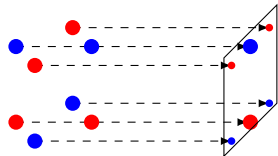


Surface perpendicular to (011)-direction

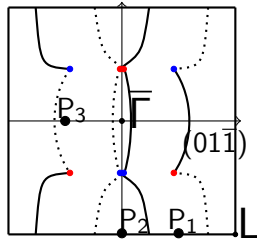
- protected surface states and Fermi arcs expected

- wave function:

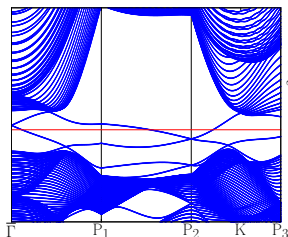
$$\psi_{n\mathbf{k}_{\parallel}}(\mathbf{R}, i\sigma) = \frac{1}{\sqrt{N_A}} A_{li\sigma}(\mathbf{k}_{\parallel}) e^{i\mathbf{k}_{\parallel} \cdot \mathbf{R}_{\parallel}}.$$



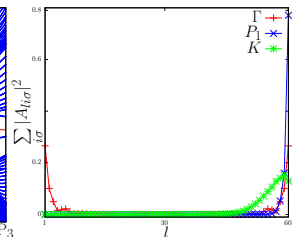
(100)



(a) surface Brillouin zone

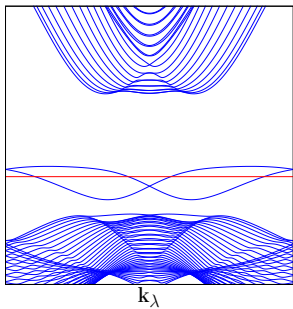


(b) surface spectrum

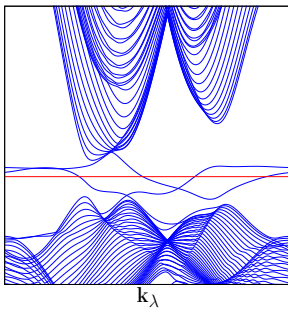


(c) probability distribution

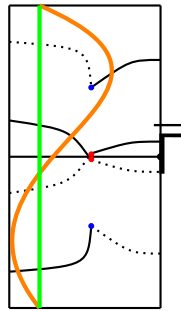
- symmetries constrain possible connectivities
- presence of more than two WP allows for new connectivities
- construction of the TWS as layers of Chern insulators



(a) trivial surface states



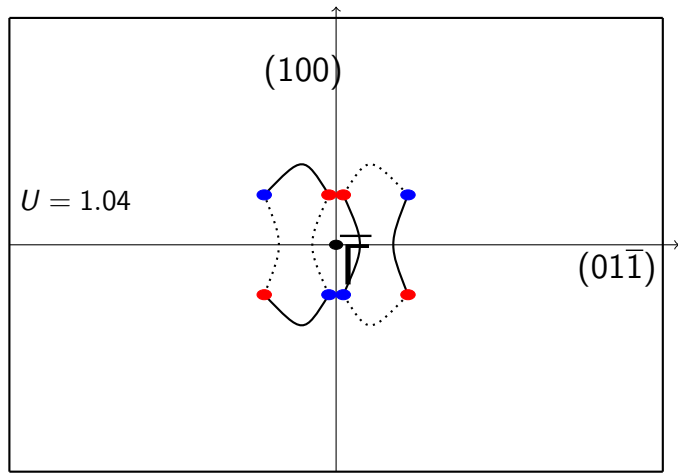
(b) protected surface states



(c)

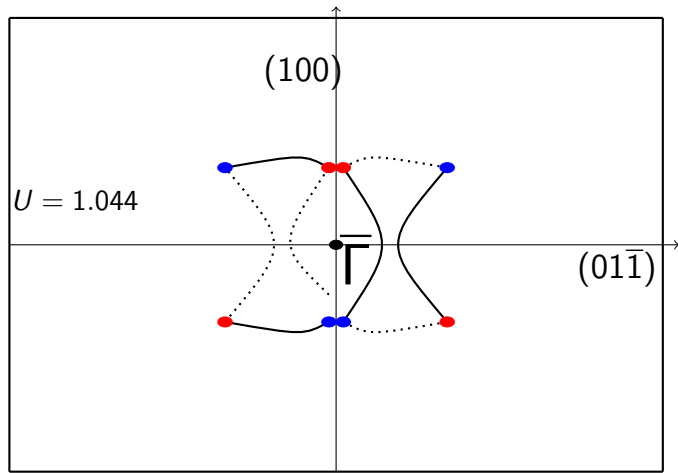
Evolution of the Fermi arcs

- connectivity depends on U , t_σ , μ , ...
- Weyl-Lifshitz transitions between different connectivities



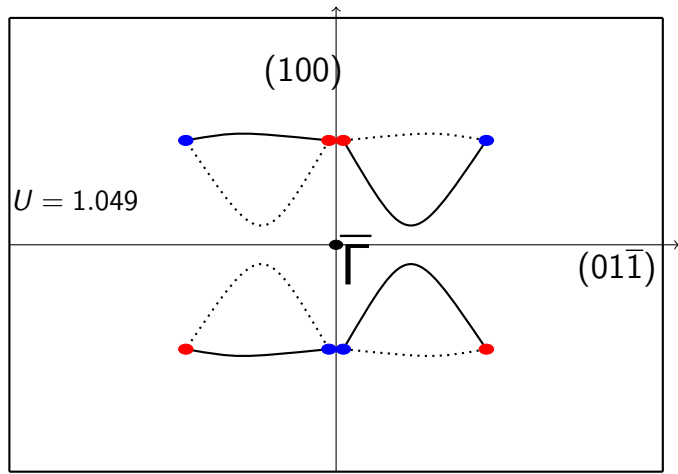
Evolution of the Fermi arcs

- connectivity depends on U , t_σ , μ , ...
- Weyl-Lifshitz transitions between different connectivities



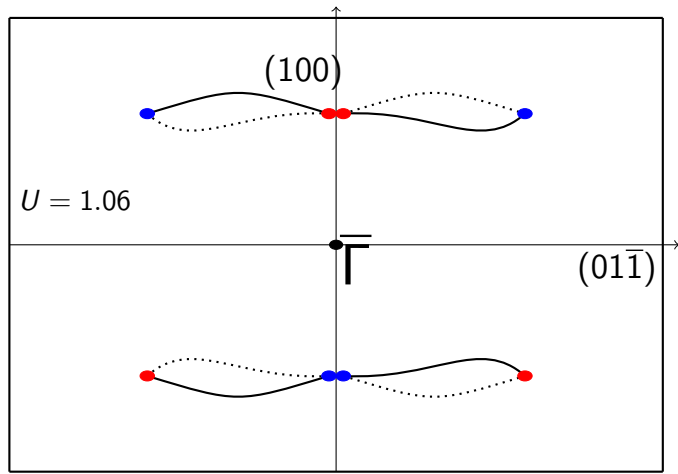
Evolution of the Fermi arcs

- connectivity depends on U , t_σ , μ , ...
- Weyl-Lifshitz transitions between different connectivities



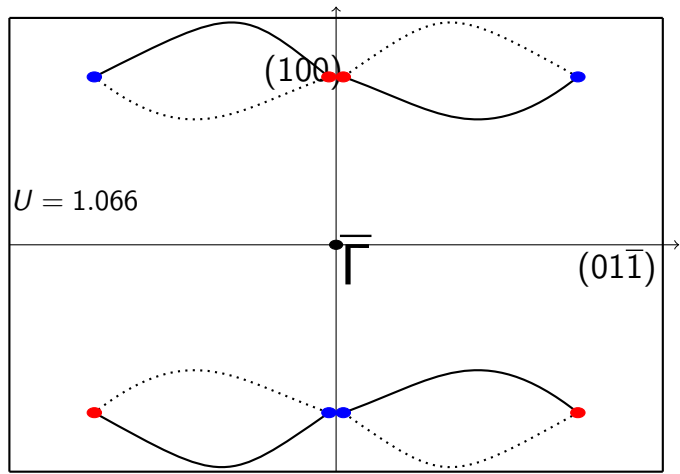
Evolution of the Fermi arcs

- connectivity depends on U , t_σ , μ , ...
- Weyl-Lifshitz transitions between different connectivities



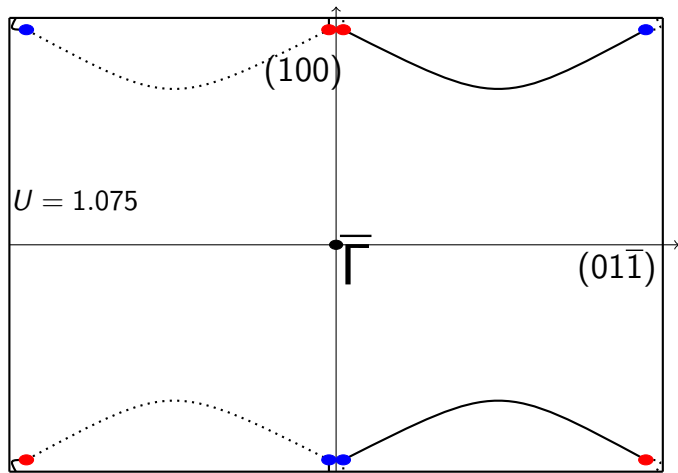
Evolution of the Fermi arcs

- connectivity depends on U , t_σ , μ , ...
- Weyl-Lifshitz transitions between different connectivities



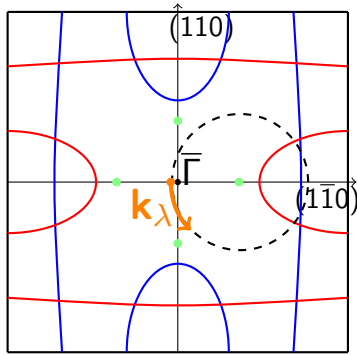
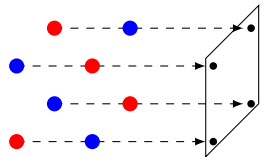
Evolution of the Fermi arcs

- connectivity depends on U , t_σ , μ , ...
- Weyl-Lifshitz transitions between different connectivities

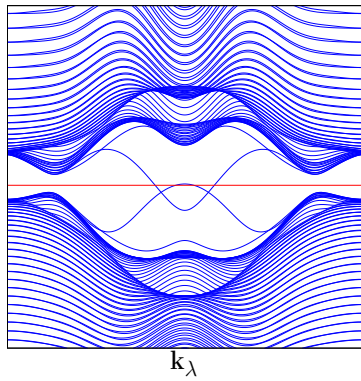


Surface perpendicular to (001)-direction

- no Fermi arcs expected

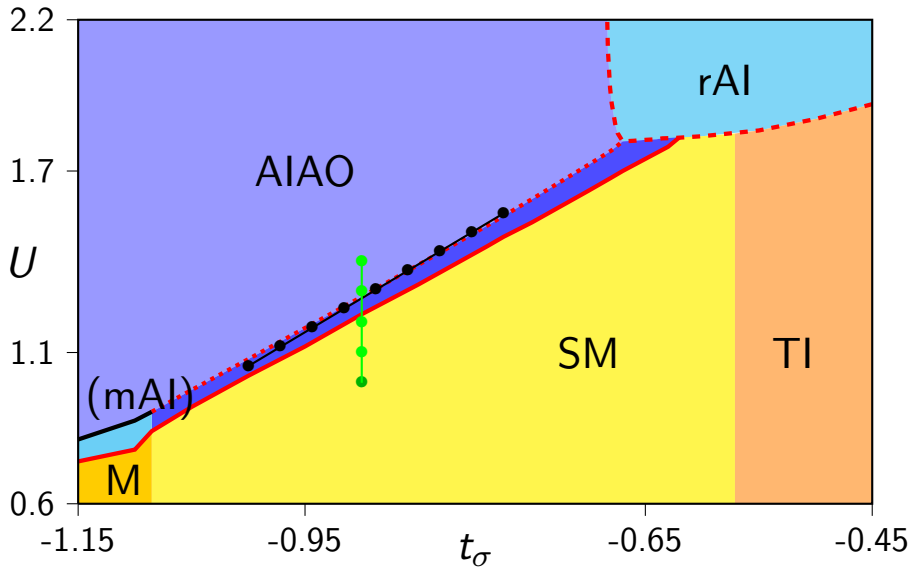


(a) surface Brillouin zone



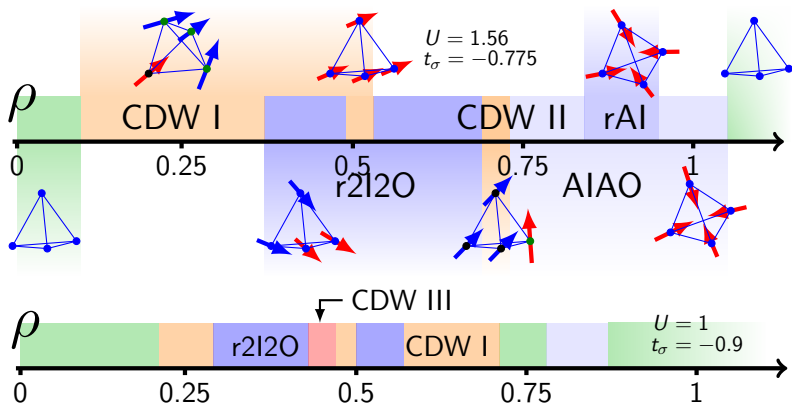
(b) spectrum

Doping



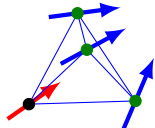
Doping: Phase diagram

- example: $\text{Y}_2\text{Ir}_2\text{O}_7 \Rightarrow \text{Y}_{2-x}\text{Ca}_x\text{Ir}_2\text{O}_7$
- charge density waves
- region with magnetic order in $U-t_\sigma$ phase diagram enlarges



Examples: CDW I & r2I2O

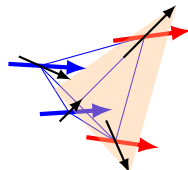
- CDW I: alternating kagomé and triangular lattices
- Weyl semimetal at half filling



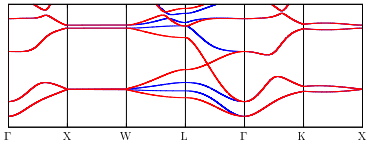
(a) CDW I



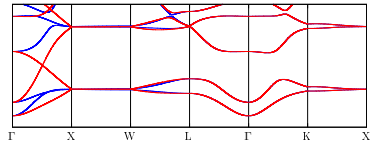
(b)



(c) r2I2O



(a) CDW I



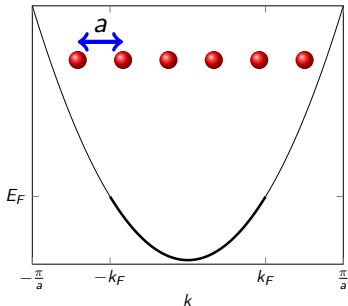
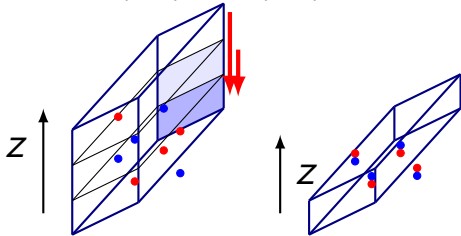
(b) r2I2O

Instabilities in TWS: Charge density waves

Idea

- CDW enlarge the unit cell
- WP can be mapped close to each other
- WP could annihilate to reduce the free energy

- Peierls Argument for 1D electron gas
- works for a gap opening at E_F
- nesting in (100)- and (111)-direction

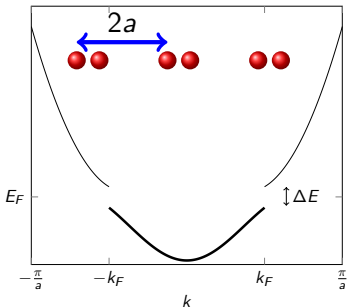
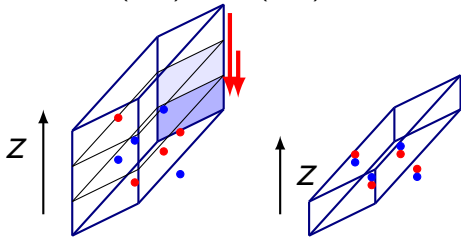


Instabilities in TWS: Charge density waves

Idea

- CDW enlarge the unit cell
- WP can be mapped close to each other
- WP could annihilate to reduce the free energy

- Peierls Argument for 1D electron gas
- works for a gap opening at E_F
- nesting in (100)- and (111)-direction



- consider larger unit cells that contain $4n$ Ir atoms and that allow for CDW in (001) and (111) direction
- calculate $16n - 1$ mean-field parameters self-consistently
- choose U and t_σ such that WP are mapped close to each other
- consider specific CDW and calculate corresponding mf-parameters
- Result: No charge density waves
- consider artificial CDW to explain this result

Ad hoc CDW in (111)-direction

- pairwise annihilation of WP on (111)-line possible
- CDW breaks symmetries of the lattice
- not all WP are at the same energy

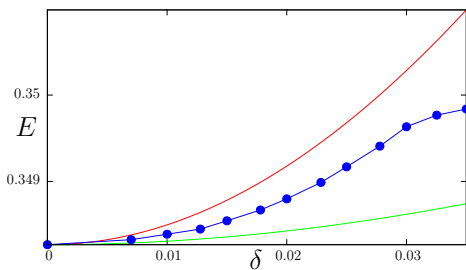
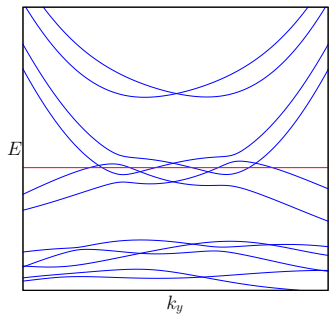
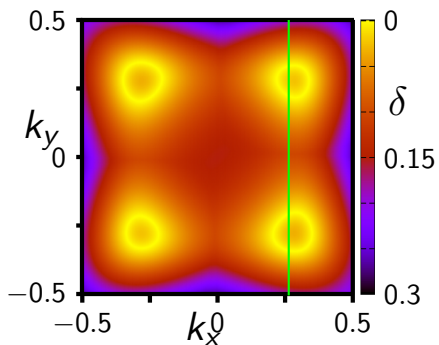
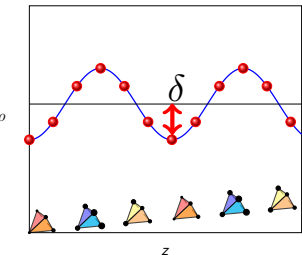


Figure: Evolution of μ and E_{WP}

- annihilation of WP never at E_F

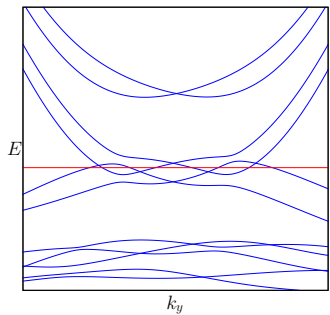
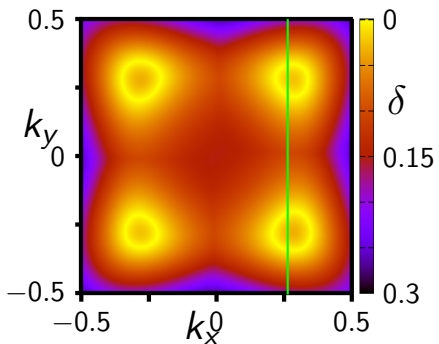
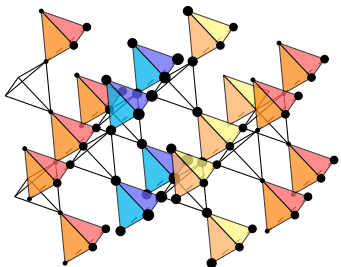
Ad hoc CDW in (001) direction

- $H_{\text{CDW}} = -U\delta \sum_i \cos\left(\frac{\pi}{n} \hat{\mathbf{e}}_z \cdot \mathbf{b}_i\right)$.
- preserves rotational symmetry
- gap closing in the plane $k_z = \pi/2n$
- emergence of 1d Fermi lines



Ad hoc CDW in (001) direction

- $H_{\text{CDW}} = -U\delta \sum_i \cos\left(\frac{\pi}{n} \hat{\mathbf{e}}_z \cdot \mathbf{b}_i\right)$.
- preserves rotational symmetry
- gap closing in the plane $k_z = \pi/2n$
- emergence of 1d Fermi lines



CDW in (001) direction: Random perturbations

- add random perturbation that breaks translational symmetry
- pairwise annihilation of WP possible
- shifts in momentum and energy
→ metal with pockets instead of insulator

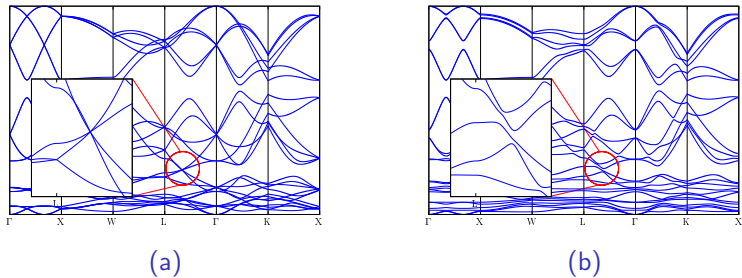


Figure: typical bandstructure for random perturbations

Summary and outlook

- $J = 1/2$ -model for pyrochlore iridates
- rich variety of phases: SM, M, TI, TWS, TWS II, AIAO, rAIAO
- Fermi arcs: different connectivities, Weyl-Lifshitz transition
- plethora of new magnetic configurations for lower densities
- Weyl semimetal at half filling
- instabilities: no CDW found
 - annihilation of WP not at E_F
 - emergence of Fermi lines
 - simultaneous shifts in momentum and energy
- To do: Analytical arguments based on low-energy effective theory

Thank you for your attention

phases at finite T

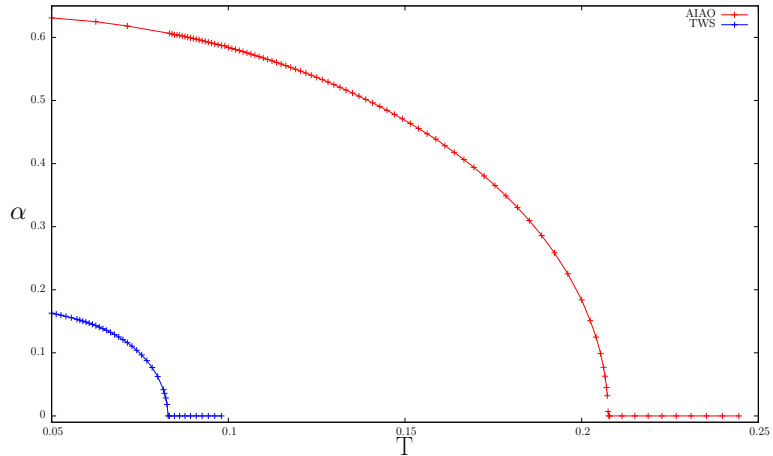


Figure: evolution of α at finite T , $t_\sigma = -0.8$

Berry flux and Berry curvature

- Berry connection/ potential for band n :

$$\mathcal{A}_n(\mathbf{R}) = i \langle n(\mathbf{R}) | \frac{\partial}{\partial \mathbf{R}} | n(\mathbf{R}) \rangle \quad (3)$$

- Berry curvature:

$$\mathbf{B}(\mathbf{R}) = \nabla_{\mathbf{R}} \times \mathcal{A} = \Omega_n(\mathbf{R}) \quad (4)$$

- Berry curvature tensor (for numerical calculations)

$$\Omega_{\mu\nu}^n(\mathbf{R}) = i \sum_{n' \neq n} \frac{\langle n | \partial H / \partial R^\mu | n' \rangle \langle n' | \partial H / \partial R^\nu | n \rangle - (\nu \leftrightarrow \mu)}{(\epsilon_n - \epsilon_{n'})^2} \quad (5)$$

- CDW in (111) direction

$$H_{\text{CDW}} = U\delta \left(n_{0\uparrow} + n_{0\downarrow} - n_{4\uparrow} - n_{4\downarrow} + \frac{1}{3} \sum_{i=1,\sigma}^3 [n_{i\sigma} - n_{i+4\sigma}] \right)$$